ISSN No. 2456-4400
Int J Med Lab Res 2026, 11(2), 15-27

IJMLR International Journal of Medical Laboratory Research

RESEARCH ARTICLE

IMMUNE RESPONSE KINETICS OF THE AFRICAN SPINY MOUSE (ACOMYS PERCIVALI) TO ENDOGENOUS SKIN COMMENSAL INFECTION: "RAPID RESOLUTION OF INFLAMMATION

JM. Kimani[1], JKN Kuria[2], S G. Kiama[1], AN. Makanya[1]

[1]*Department of Veterinary Anatomy and Physiology, University of Nairobi, Nairobi, Kenya*
[2]*Department of Department of Veterinary Pathology, Microbiology and Parasitology, University of Nairobi, Nairobi, Kenya*

Received: 07 August, 2026 /Revision: 15 August, 2026 /Accepted: 27 August, 2026

ABSTRACT: The African spiny mouse is a premier mammalian model for scarless cutaneous regeneration. This investigation characterized how its endogenous skin commensals influence acute host immunity, a crucial determinant of tissue repair outcome. Analysis of the dorsal auricular flora identified dominance by a native Coagulase Negative-Novobiocin-Sensitive Staphylococcus (CoNS-NSS) strain. Intradermal challenge with this resident strain elicited an instantaneous, high-magnitude inflammatory response, characterized histologically by subtle cutaneous small vessel vasculitis and fibrin deposits, features pathognomonic for the Arthus reaction. This atypical immediate onset compared to other studies we hypothesize that Acomys percivali maintains a systemic reservoir of high-titer, pre-existing antibodies against staphylococcal antigens, potentially mediated by commensal superantigens influencing local immunity. Quantitative analysis confirmed an accelerated resolution program: neutrophils and macrophages peaked at day 1, followed by statistically significant clearance of macrophages and T-cells by day 14. This rapid inflammatory withdrawal facilitates the complete regression of transient fibroplasia, establishing that controlled, rapidly resolved immune-complex-mediated inflammation dictates scarless regeneration in this species.

Key words: Acomys percivali, Regeneration, Coagulase Negative-Novobiocin-Sensitive Staphylococcus (CoNS-NSS), immune-complex-mediated inflammation, vasculitis.

Corresponding Author:
Dr. John M. Kimani,
Department of Veterinary Anatomy and Physiology, University of Nairobi, Nairobi, Kenya.
Email:jmuturik@uonbi.ac.ke

INTRODUCTION:

The skin serves as a vital protective interface against mechanical injury, environmental insults, and microbial invasion. Structurally, it comprises the epidermis, dermis, and hypodermis, each housing distinct cell populations. The epidermis is dominated by keratinocytes reinforcing the physical barrier, alongside immune cells such as Langerhans cells and dendritic epidermal T-cells [1,2]. The dermis is rich in extracellular matrix, fibroblasts, mast cells, and both myeloid and lymphoid immune cells[3]. Extensive crosstalk between epithelial, stromal, and immune cells regulates skin immunity and maintains tissue homeostasis[2,3].

A diverse microbial community constantly colonises the skin's surface and appendages, interacting with host cells to influence local and systemic immunity[4-7]. Many of these organisms are commensals that cause no harm unless the immune status is compromised[8]. Studies in conventional laboratory mice have identified numerous bacterial genera, with *Staphylococci* particularly coagulase-negative species (CoNS) being predominant[9,10].

When the skin barrier is breached by injury or disease, opportunistic microorganisms initiate a complex immune cascade involving antigen-presenting cells such as dendritic cells, macrophages, and keratinocytes, which activate innate and adaptive immune effector responses[11-14]. This typically recruits neutrophils, monocytes, and NK cells, followed by T-cell involvement in antigen neutralisation.

Although skin repair aims to restore normal structure and function, adult mammals typically undergo an imperfect process characterised by chronic inflammation and permanent scar formation. A notable exception is the genus *Acomys*, which possesses the rare mammalian trait of healing skin wounds rapidly and without scarring, regenerating all cutaneous structures including hair follicles and cartilage[15,16]. The outcome of wound repair, fibrosis or regeneration is fundamentally influenced by the immune response[17-19]. Mechanistic studies suggest that *Acomys* processes injury differently from non-regenerating rodents: it demonstrates substantially lower and more rapidly declining neutrophil levels, and a reduced release of pro-inflammatory cytokines such as IL-6, CCL2, and CXCL1[20-22]. These findings indicate that the temporal regulation and resolution of inflammation not merely its magnitude are paramount to achieving scarless healing.

Intradermal infection studies have further shown that commensals such as *S. epidermidis* induce a distinct, commensal-specific T-cell response associated with immunoregulation, and that inflammatory monocytes can respond to commensal-derived ligands to limit tissue damage[23-26]. Despite the acknowledged role of both inflammation and resident microbiota in shaping repair outcomes, the precise immunological dynamics elicited by skin commensals following an intradermal breach remain poorly defined in regenerative species.

This study addressed that gap using wild-caught *A. percivali* to investigate host-commensal interactions using the animal's native flora. The objectives were to isolate and phenotypically identify the predominant resident bacteria of the dorsal auricular skin, and to characterise the spatio-temporal kinetics of the immune response specifically neutrophils, macrophages, and T-cells following intradermal inoculation with the dominant Coagulase Negative-Novobiocin-Sensitive *Staphylococcus* (CoNS-NSS) strain.

MATERIALS AND METHODS:

Experimental Animals and Ethical Compliance

African spiny mice (*A. percivali*) were captured live using Sherman traps baited with peanut butter and oats at the Mpala Ranch in Laikipia County, Kenya. Trapping was conducted under the authority of Kenya Wildlife Services (KWS) license reference No. KWS/BRM/5001. A total of 90 animals were used for initial microbiological

sampling. Trapped animals were subsequently housed in steel wire mesh cages in the Department of Veterinary Anatomy and Physiology at the University of Nairobi. Housing conditions were designed to simulate the natural environment, maintaining a 12/12h light-dark cycle at room temperature, with food and water provided *ad libitum*. All animals were allowed a minimum 14-day acclimatization period before the initiation of infection studies.

All animal procedures adhered to protocols approved by the University of Nairobi, Faculty of Veterinary Medicine, Biosafety, Animal Care and Use and Ethics Committee. This research was authorized by National Commission for Science, Technology and Innovation (NACOSTI) under license number: NACOSTI/P/25/4182558.

Microbiological Sample Collection, Isolation and Colony counts

Microbiological transport swab (IMPROSWAB, Guangzhou improve Medical Instruments Co. Ltd) were opened aseptically. Skin swabs were collected aseptically from the dorsal pinnae (ear skin) of the 90 animals immediately post-trapping, ensuring samples were taken from non-overlapping areas. Swabs were immediately placed in transport media (Stuart media, Guangzhou improve Medical Instruments Co. Ltd) and refrigerated in a cool box for transport to the microbiology laboratory. Upon arrival, the swabs were vortexed in Tryptone Soy Broth (TSB) and incubated at 37°C for 12 hours. Isolates from the TSB were then serially diluted up to a 10^{-3} dilution and seeded onto petri dishes containing Plate Count Agar (PCA) and Blood Agar to facilitate the identification of different colonial morphologies. The seeded petri dishes were further incubated at 37°C for 12 hours.

Phenotypic Identification of Staphylococcus spp.

Identification began with Gram staining of selected colonies to evaluate purity and classify cellular morphology. Isolates were classified into Gram positive cocci, Gram positive rods, and Gram-negative rods. The most abundant group, Gram positive cocci, was then subjected to specific biochemical characterization tests necessary to differentiate Coagulase Positive *Staphylococci* (CoPS, such as *Staphylococcus aureus*) from Coagulase Negative *Staphylococci* (CoNS). The differentiation battery included the tube Catalase test, Mannitol Salt Agar (MSA) Test, DNase test, the gold standard Coagulase Test, and the Novobiocin Test as documented in diagnostic microbiology [27,28]

Inoculum Preparation and Intradermal Inoculation

A single strain belonging to the majority group, identified phenotypically as Coagulase Negative-Novobiocin Sensitive *Staphylococci*, was chosen for the inoculation phase of the study. The concentration of bacteria was quantified by assessing Colony-Forming Units (CFUs) via serial dilutions and standard plate count methods. Based on pre-testing, an infective dose of 1 x 10^6 CFU was calculated.

Before conducting the actual infection study a pretest was run for a month. For the infection study, five *A. percivali* mice were allocated to each of the four time points: Day 1, Day 3, Day 7, and Day 14. Anesthesia was induced using 5% (v/v) isoflurane in an induction chamber, which was sterilized between inoculations to prevent cross-contamination. The middle of the right pinna was inoculated intradermally with 10 µl containing the 1 x 10^6 CFU strain, adjusted in Phosphate Buffer Saline (PBS, pH 7.2). The middle of the left pinna received a 10 µl injection of PBS alone to serve as the control.

Morphological and Histopathological Analysis

Five adult animals per time point (Days 1, 3, 7, and 14 post-inoculation) were used for histological processing. Mice were sacrificed after overdosing with isoflurane at the predetermined time points (Days 1, 3, 7, and 14 post-inoculation). A pre-test involved observing for changes in extracellular matrix, different immune cells types, cell numbers at the peak of acute inflammation (Days 1-5) daily in HE sections for with CoNS-NSS-inoculated and PBS-inoculated sites. Then examining the same parameters for stalled chronic inflammation and injury site matrix remodeling on days 7, days 14

and days 21(29). Animals were exposed to 4%(v/v) vaporised isoflurane inhalation anaesthetic (ISOTROY 250, manufactured by Troikaa pharmaceuticals Ltd, Gujarat, India) in a closed trasparent induction chamber attached to Veterinary Anaesthesia Machine(Surgivet, Smiths Medical, ASD, inc. USA) to allow easy monitoring of the animal and control of isoflurane concentration. Completely sleep anaethesized animal was euthenised by cervical dislocation. The infected (right) and control (left) pinnae were immediately collected by excision, fixed in 10% Neutral Buffered Formalin, and subsequently processed for paraffin embedding. The pinna tissues were cut into halves along the proximal-distal axis and embedded in transverse orientation in paraffin blocks.

The tissues were cut at a thickness of 5 µm using a *Leitz Wetzlar*, Rotary microtome. The sections were stained with hematoxylin-eosin (HE) and observed under a Leica® DM500 light microscope at magnifications of x40 and x100 objectives. Micrographs of histological serial sections captured in a light microscope were analyzed with the Leica application suite software (Switzerland). Leica application suite software (Switzerland) has an integrated digital measuring tool, and it was used to affix the scale bars. Adobe Photoshop and Illustrator were used for image editing and labeling.

Immunohistochemical (IHC) Analysis

Immunohistochemistry was performed to identify and quantify specific leukocyte populations at the inoculation sites. The following primary antibodies from Medaysis, USA were used: Mouse Anti-CD45 (LCA) for total leukocytes; Mouse Anti-CD3 for T-cells; and Mouse Anti-Macrophage L1 Protein (Mac387) for macrophages.

The IHC protocol involved standard procedures: deparaffinization, rehydration, blocking of endogenous peroxidase with 3% H_2O_2 for 10 min, and enzymatic treatment with 2% trypsin for 10 min. Non-specific binding was mitigated using a blocking solution (PBS and 10% normal goat serum). Sections were incubated sequentially with primary antibodies (30 min) (With the following dilution rations LCA1:500, CD3 1:500 and L1 Protein1:500), washed, and then incubated with secondary antibodies diluted 1:1000. Detection was achieved using EnVision kits (Avidin, Biotinylated horseradish peroxidase Complex), followed by application of the substrate, diaminobenzidine tetra hydrochloride (DAB), for 5–10 minutes. Slides were lightly counterstained with hematoxylin. Positive control tissues utilized were T-cell lymphoma tissue (for CD3) and lymph node tissue (for CD45 and Mac387). Images of fields were captured using a digital camera mounted on a Leica ® DM 500 microscope (Switzerland) and analyzed with the Leica application suite. Leica application suite software (Switzerland) has an integrated digital measuring tool, and it was used to affix the scale bars. Adobe Photoshop and Illustrator were used for image editing and labeling.

Morphometric and Statistical Analysis

From the two paraffin blocks per pinnae (per animal in a timepoint), 10-15 histological serial sections were stained. Three images were captured from each histological serial section using the Leica Application Suite software (Switzerland). Leica application suite software (Switzerland) includes an integrated digital measuring tool. Images taken at x100 objective magnification and affixed with scale bar in microns (µm) were used for counting cells. Using *ImageJ* count-tool grid, the number of neutrophils (HE stained) and immunopositive cells (CD45, CD3, and Mac387) were counted from the captured images. Raw data of the counts were entered into an Excel sheet. Descriptive statistics, means, and Standard Deviation (SD) were calculated.

Quantitative data were expressed as Mean ± Standard Deviation (SD). Statistical significance of cell counts at different time points was assessed using repeated measures Analysis of Variance (ANOVA). A P-value threshold of 0.05 was established for statistical significance. Statistical analysis and graph generation were performed using Stata/MP 14.2 software.

RESULTS:

Diversity of Skin-Resident Bacterial Communities

Analysis of the 90 microbiological samples collected from the dorsal auricular skin revealed a predominant Gram-positive flora. Gram positive cocci were the most frequently isolated group, followed by Gram positive rods/bacilli, and finally Gram-negative rods/bacilli **(Table 1)**.

Table 1: Diversity of Skin-Resident Bacterial Isolates in *Acomys percivali* (n=90)

Cellular morphology	Number of isolates	Frequency (%)
Gram positive cocci	66	73.3
Gram positive rods/bacilli	36	40.0
Gram negative rods/bacilli	29	32.2

From the 90 swabs, a swab could contain a combination of Gram-positive cocci, Gram positive rods/bacilli and Gram-negative rods/bacilli isolate.

Phenotypic Characterization of Dominant *Staphylococcus* Species

Focusing on the 66 Gram positive cocci isolates, further phenotypic characterization confirmed that Coagulase-negative *Staphylococci* (CoNS) outnumbered Coagulase-positive *Staphylococci* (CoPS), with only 30.3% of isolates testing positive for the Coagulase Test. The most frequently isolated and dominant staphylococcal species were identified as Coagulase-Negative, Novobiocin–Sensitive *Staphylococci* (CoNS-NSS), accounting for 60.61% of the isolates tested for Novobiocin sensitivity **(Table 2)**. This CoNS-NSS strain was subsequently selected for the intradermal inoculation studies.

Table 2: Phenotypic Characterization of Dominant *Staphylococcus* Species Isolates (n=66)

Test conducted	Number of isolates screened	Number of positive isolates	Positivity Rate (%)
Catalase Test	66	64	96.6
Yellow colonies in MSA	66	9	13.3
Clear zone in DNase Agar	66	11	16.67
Coagulase Test	66	20	30.3
Novobiocin Test (Diameter Zone > 16)	66	40	60.61

Histopathological Findings Post-Inoculation

Intradermal inoculation of the resident CoNS-NSS strain induced a rapid, intense, but temporally confined immuno-inflammatory response.

At Day 1 post-infection, the histological profile was characterized by immune-complex-like inflammation (acute dermatitis). This involved subtle cutaneous small vessel vasculitis (CSVV), highlighted by hyperemia (engorgement of blood vessels), endothelial swelling, and dense perivascular cuffing predominantly composed of neutrophils **(Fig. 1).** Control pinnae injected with PBS showed only vessel engorgement with little or no inflammatory infiltrate at day 1**(Fig. 1).**

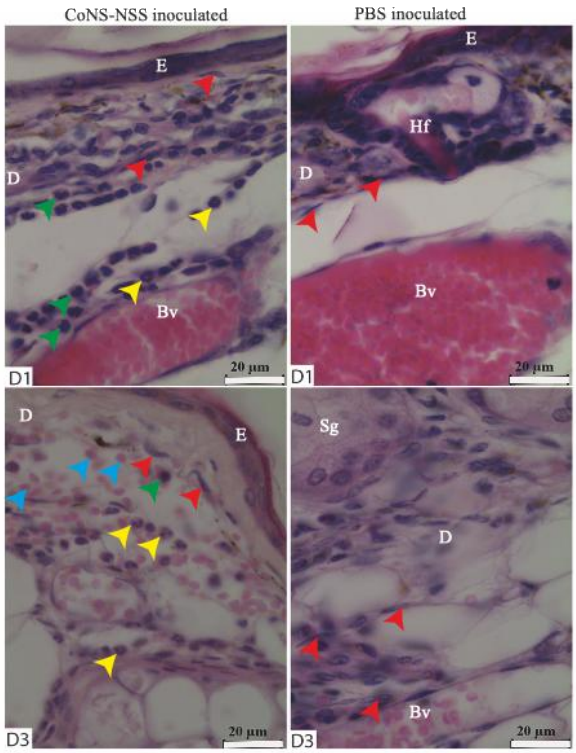

FIG. 1. Histopathology profiles of skin lesions at site of Coagulase Negative-Novobiocin-Sensitive *Staphylococcus* (CoNS-NSS) innoculation and ears inoculated with saline (PBS) (control) at D1 and D3. At D1 post-infection there was a immune-complexes-like inflammation (acute dermatitis) denoted by vasculitis highlighted by hyperemia (engorgement of blood vessels with blood), endothelial swelling and high cuff-like perivascular accumulation of leucocytes (predominantly neutrophils), PBS-treated ears only showed engorgement of blood vessels with little or no inflammatory infiltrate. At D3 post-infection vasculitis was marked by infiltration of neutrophils, extravasation of erythrocytes (without hemolysis suggesting an increased vascular permeability due to reduced endothelial integrity) and fibrin deposits in the dermis. There was also edema accompanying influx of neutrophils numbers. E-Epidermis, D-Dermis, Sg-Sebaceous gland, Bv - Blood

vessel, blue arrowheads- Extravasated Erythrocytes/erthrodiapedesis, yellow arrowheads-Neutrophils, green arrowheads -Macrophages, Red arrowheads - Fibroblast Bars =20µm

By Day 3 post-infection, the inflammatory response peaked, exhibiting the characteristic histologic features of the Arthus reaction. This response was marked by severe vasculitis, robust infiltration of neutrophils, extravasation of erythrocytes (*erythrodiapedesis*), indicative of compromised endothelial integrity and increased vascular permeability), and substantial fibrin deposits within the dermal layer **(Fig. 1).**

Following this acute phase, a sharp decline in inflammatory infiltrate was observed. By Day 7, the injury site entered a transient phase of fibroplasia, denoted by the proliferation of fibroblasts **(Fig. 2).** Crucially, by Day 14, this transient fibrosis had regressed completely **(Fig. 2).** Cellular proliferation decreased dramatically, and the infected site was histologically comparable to the control skin, demonstrating complete resolution of the inflammation and pathology.

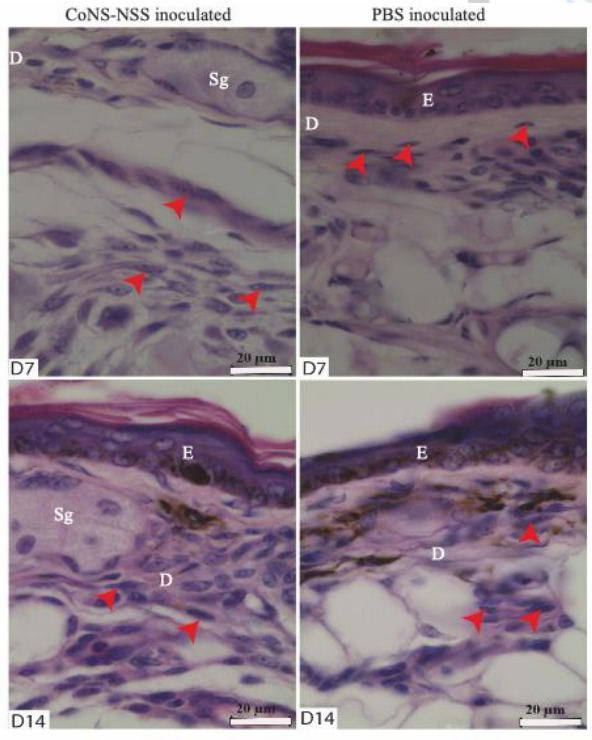

FIG. 2. Histopathology profiles of skin lesions at site of Coagulase Negative-Novobiocin-Sensitive *Staphylococcus* innoculation and ears inoculated with saline (control) at D7 and D14. The healing of the infection went through a transient dermal remodeling phase that is marked by proliferation of fibroblasts as indicated at day 7**(D7)** post infection. Laying down of extracellular matrix then regresses and proliferation of cells decreases and becomes extremely low at day 14**(D14)** and the infection site is comparable to PBS-treated skin. E-Epidermis, D-Dermis, Sg-Sebaceous gland. Red arrowheads - Fibroblast Bars =20µm

Immunohistochemical analysis at the site of intradermal Innoculation.

The nature of the immuno-inflammatory cell response at the site of bacterial infection in the ear pinna was analysed by immunohistochemistry between days 1 and 14 post-inoculation with CoNS-NSS strain. Leukocytes were identified by expression of surface antigen profiles: CD45 (total leucocytes), CD3 (T-cells) and Mac387 (macrophages) at different times points post inoculation **(Fig. 3, Fig. 4).** There was a rapid and transient increase in macrophage numbers reaching a peak at day 1 **(Fig. 3).** There was then a sharp decline in numbers of macrophages in the inflammatory infiltrate all the way to day 14**(Fig. 4).** Total leukocyte (CD45+) and T-lymphocyte (CD3+) numbers were highest on day 3 and then showed a steady decline **(Fig. 4).**

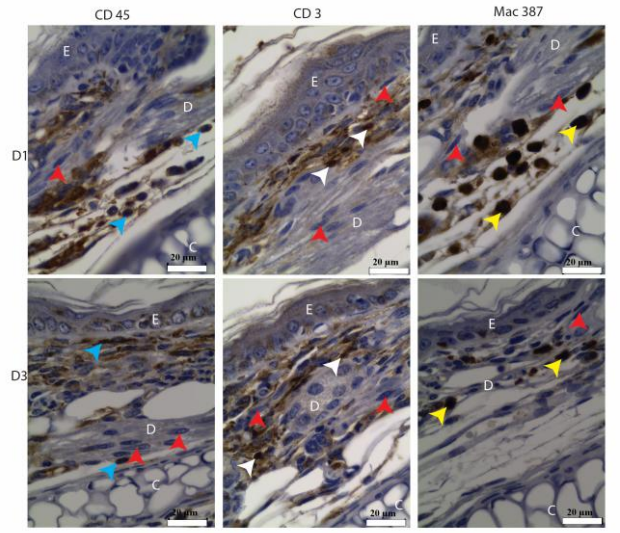

FIG. 3. Immune response to commensal Coagulase Negative-Novobiocin-Sensitive *Staphylococcus* intradermal infection at days 1 and 3 post-infection. Leukocytes were identified by immunohistochemistry by expression of surface antigen profiles (CD45, CD3 and Mac387). There was a rapid and transient increase in macrophage (Mac387+ cells) numbers reaching a peak at day 1 post infection. There was an increase in total leukocytes ($CD45^+$ cells) in the infiltrate at the site of skin inoculation up to day 3. T-cell ($CD3^+$cells) numbers were highest on day 3 post-infection. E-Epidermis, D-Dermis,C-Cartilage, Red arrowheads -

Fibroblast, blue arrowheads-CD45$^+$ cells, white arrowheads-CD3$^+$cells, yellow arrowheads-Mac387$^+$ cells Bars= 20 µm

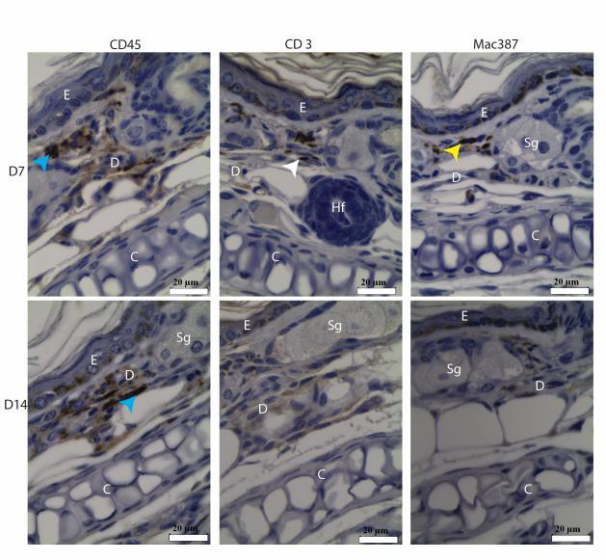

FIG. 4. immune response to commensal Coagulase Negative-Novobiocin-Sensitive *Staphylococcus* intradermal infection at days 7 and 14 post-infection. Leukocytes were identified by immunohistochemistry by expression of surface antigen profiles (CD45, CD3 and Mac387). There was a sharp decline in numbers of macrophages (Mac387+ cells) in the inflammatory infiltrate through day 14. CD45$^+$ cells and CD3$^+$cells remained relatively low at the site of skin inoculation from days 7 to 14. CD45$^+$ cells (blue arrowheads) CD3$^+$cells (white arrowheads) Mac387$^+$cells (yellow arrowheads) Bars= 20 µm

Kinetics of leukocyte infiltration

Quantification of neutrophils from HE-stained sections showed a rapid influx, peaking at Day 1 post-inoculation with CoNS-NSS strain **(Table 3)**. The mean neutrophil count at Day 1 was 19.8 ± 7.8 cells per 100x field **(Table 3)**. This count decreased by Day 3 (14.0 ± 5.8) and had nearly vanished by Day 7 (0.7 ± 0.7), demonstrating an exceptionally acute and transient innate inflammatory phase **(Table 3)**.

Table 3: Quantification of Neutrophil Infiltration Post-Inoculation (Cells/100x Field)

Time Point	Mean Count	Standard Deviation (SD)
Day 1	19.8	7.8
Day 3	14.0	5.8
Day 7	0.7	0.7

IHC analysis confirmed distinct kinetics for macrophages, total leukocytes, and T-cells **(Fig. 5).**

Macrophages (Mac387+): Macrophages exhibited the earliest cellular peak, reaching maximum numbers at Day 1 (15.13 ± 3.09). Following this peak, there was a statistically significant sharp decline in macrophage presence, persisting through Day 14 (4.17 ± 1.47) **(Table 4)**

Table 4: Spatio-Temporal Kinetics of Leukocyte Populations (Immunopositive Cells/1000x Field).

Marker	Day 1 Mean ± SD	Day 3 Mean ± SD	Day 7 Mean ± SD	Day 14 Mean ± SD	P-value
CD45 (Total Leukocytes)	13.40± 1.52	19.80± 2.77	11.22± 3.46	6.67± 2.18	0.693
CD3 (T-cells)	7.00± 3.34	13.43± 1.90	8.33± 1.58	6.50± 2.07	0.000
Mac387 (Macrophages)	15.13± 3.09	13.00± 4.55	8.71± 2.75	4.17± 1.47	0.000

Statistical significance of cell counts at different time points was assessed using repeated measures Analysis of Variance (ANOVA). A P-value threshold of 0.05 was established for statistical significance.H_o:No signicant differences in means across repeated Measurement. CD3 (T-cells) and Mac387 (Macrophages) cell counts was significantly different across different time points.The assumption is that A.percivali is one species with the same genetic makeup.

Total Leukocytes (CD45+) and T-cells (CD3+): Total leukocytes (CD45+) and T-cells (CD3+) peaked slightly later, both reaching their highest recorded numbers at Day 3 post-infection **(Table 4)**. CD45+ cells peaked at 19.80 ± 2.77, while CD3+ cells peaked at 13.43 ± 1.90 **(Table 4)**. The T-cell population demonstrated a significant decrease over the subsequent days, falling to 6.50 ± 2.07 by Day 14. CD45+ numbers also showed a steady decline after Day 3, reaching 6.67 ± 2.18 by Day 14 **(Table 4)**.

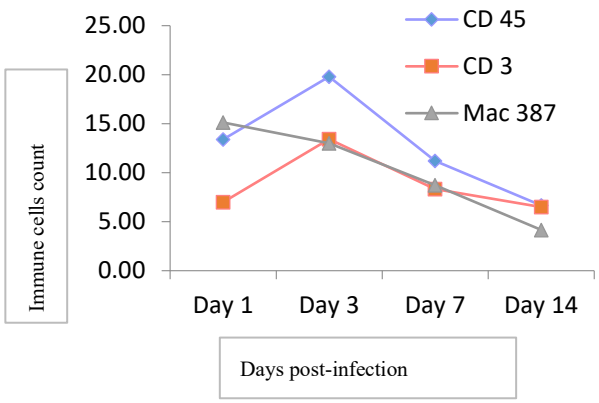

FIG. 5. Graphical representation of immune cells counts at different time points post intradermal infection immune response to commensal Coagulase Negative-Novobiocin-Sensitive *Staphylococci*us intradermal infection at Days 1 and 3 Post-infections. Leukocytes were identified by immunohistochemistry by expression of surface antigen profiles (CD45, CD3& Mac387). There was a rapid and transient increase in macrophages (Mac387+cells) numbers reaching a peak at day 1 post infection. There was Increase in total leukocytes ($CD45^+$ cells) in the infiltrate at the site of skin inoculation upto day 3. T-cells ($CD3^+$cells) numbers were highest on Day3 post-infection.

DISCUSSION:

Laboratory mice, including transgenic and knock-out strains, are the most commonly used models in cutaneous biology and wound healing research. However, most infection studies employ human-derived bacterial strains in laboratory mice to which they are foreign. Wild rodent species, though used infrequently, are valuable because disease processes occur naturally or can be induced under realistic conditions[30]. Little is known about the bacterial species inhabiting the skin of wild mice across different environments. Since microbial colonisation can significantly affect study outcomes[31-32], identifying the resident bacterial populations of murine skin under natural conditions is important for understanding their influence on cutaneous research.

This study used wild *A. percivali* a species capable of complete skin regeneration including adnexa and cartilage[15,16], to determine the dominant native skin bacteria and the immune cellular dynamics that follow intradermal inoculation with those same bacteria in the ear pinna.

The finding that wild *A. percivali* skin flora is overwhelmingly dominated by Gram-positive cocci (73.3%), specifically *Staphylococcus* species, is consistent with established observations in both laboratory mice and human cutaneous biology[10-33]. These findings mirror those reported for C57BL/6 and heterogeneous intercross line mouse strains. Gram-negative bacteria, though rarely detected on normal skin, have been reported as predominant in some superficial swab studies of in superficial skin swabs of C57BL/6 and heterogeneous intercross line mice strains [34-36], and the inconsistencies between studies remain unresolved. Differences observed may reflect variations in sampling location, host genetic background, or the distinct environmental conditions of wild *A. percivali*.

Further characterisation identified the dominant strain as Coagulase-Negative, Novobiocin-Sensitive *Staphylococci* (CoNS-NSS), consistent with *Staphylococcus epidermidis*, a ubiquitous human skin commensal[37].This contrasts with murine studies identifying Novobiocin-Resistant CoNS as predominant[9,10]. *S. epidermidis* has been identified as the majority isolate from 11 wild mice species [38]. The use of wild-caught animals and their native flora addresses a key methodological limitation in cutaneous studies, where foreign pathogens may obscure true host-commensal interactions. Future genomic sequencing will provide a more accurate taxonomic profile of *A. percivali* skin communities.

Inflammation and immunity fundamentally influence whether repair results in regeneration or fibrosis[17,39,40]. Intradermal inoculation with the dominant CoNS-NSS strain produced acute dermatitis marked by subtle cutaneous small vessel vasculitis, perivascular neutrophilic cuffing, erythrodiapedesis, and dermal fibrin deposits the definitive histological features of a Type III hypersensitivity (Arthus) reaction[41-43]. This immune complex-mediated inflammation involves deposition of Ig-based immune complexes, whose immunopathogenesis encompasses mechanisms such as molecular mimicry, Toll-like receptor activation, and superantigen activity (Cartin-Ceba

et al., 2010; Muñoz-Grajales and Pineda, 2015). In *Staphylococci*-related vasculitis specifically, Staphylococcal protein A (SpA), a B-cell superantigen, is the primary implicated mechanism[46,47]. immune complexes (ICs)-activated neutrophils undergo transmigration, trigger further IC formation, and initiate acute inflammation characterised by massive neutrophil influx, oedema, erythrodiapedesis, and vasculitis [48-50]. The deposition of immune complexes (ICs) can occur on both the luminal and abluminal sides of blood vessels [51,52]. Resolution then proceeded through a transient fibroplasia phase, which subsequently regressed completely by Day 14, mediated via apoptosis and macrophage-driven clearance.

Crucially, the classical Arthus reaction requires pre-existing high-titer circulating antibodies. The immediate onset of IC-mediated vasculitis in *A. percivali* upon the *first* intradermal injection of its own resident CoNS-NSS strain is highly unusual and we hypothesize that the spiny mouse maintains a significant systemic antibody pool against staphylococcal antigens. This contrasts with prior studies where rabbits and mice required intravenous pre-treatment with human IgG to develop characteristic Arthus histology[42,53]. The data strongly support the hypothesis that the resident CoNS-NSS strain possesses Superantigen properties, driving robust antibody production and rapid IC formation. SAg genes have been increasingly identified in various CoNS isolates, and CoNS-derived SAgs have been implicated in cutaneous leukocytoclastic vasculitis in humans [54-56]

This rapid, potent inflammatory peak (Days 1–3) is central to understanding the *Acomys* regenerative phenotype. Although inflammation is often viewed as antagonistic to regeneration, the data reveal that the intense, localised response is immediately followed by a steep and statistically significant decline in all major immune cell populations. The SAg-driven acute response likely serves as a highly efficient mechanism for rapid antigen and cellular debris clearance[57]. By achieving maximum inflammatory magnitude quickly and then initiating an accelerated resolution programme, the host minimises the duration of sustained inflammation the established prerequisite for fibrosis and scarring.

The sequential leukocyte kinetics further illuminate *Acomys* resolution strategy. Macrophages peaked concurrently with neutrophils at Day 1, suggesting timely mobilisation for phagocytic clearance of immune complexes and apoptotic neutrophils. Total leukocytes and T-cells peaked slightly later at Day 3, confirming adaptive immune involvement consistent with commensal-driven T-cell activation described in other studies[24-26]. Both macrophage and T-cell populations then showed sharp, statistically significant declines through Day 14.

This immune withdrawal programme is critical for tissue fate determination. The transient fibroplasia observed at Day 7, which resolved completely by Day 14, provides direct histological evidence of successful regeneration. Persistent inflammation prolongs fibroblast activation and extracellular matrix deposition, leading to fibrosis[58]. The complete regression of fibroplasia correlates directly with macrophage-mediated immune cell clearance[59], demonstrating that controlled kinetics of inflammatory resolution are the essential determinant allowing tissue to shift from fibrotic repair toward regeneration.

CONCLUSIONS:

This study successfully characterized the indigenous microbiota of wild *Acomys percivali* dorsal auricular skin and provided a detailed spatio-temporal analysis of the acute immune response to intradermal commensal challenge. The resident skin flora of *A. percivali* is dominated by Gram positive cocci, specifically Coagulase-Negative, Novobiocin-Sensitive *Staphylococci*. Intradermal inoculation of the resident strain triggers a rapid, high-magnitude, yet highly transient inflammatory response characterized by the definitive histological features of an Arthus reaction (immune-complex-mediated vasculitis). The instantaneous nature of

this Type III hypersensitivity we hypothesize that *A. percivali* maintains high, pre-existing systemic antibody levels against resident staphylococcal antigens, providing a state of perpetual immune preparedness, likely mediated by commensal Superantigen activity.

The immune response is defined by an exceptionally rapid acute phase (neutrophil and macrophage peaks at D1, T-cell peak at D3) followed by accelerated, statistically significant immune cell clearance and withdrawal. This rapid resolution program facilitates the complete regression of transient fibroplasia observed at D7, confirming that the tight control over the duration of inflammation is critical to achieving complete cutaneous regeneration in *Acomys*.

Acknowledgement

We would like to acknowledge financial support from National Research Fund, Kenya (NRF). They would also like to thank John Ewoi (*Posthumous*) and Alois Wambua for helping in live-trapping of the *A. percivali* mice in Mpala Ranch. We thank Stanely Marete for husbandry assistance and care for *A. percivali*

REFERENCES:

[1]. Brandner JM. Tight junctions and tight junction proteins in mammalian epidermis. Eur J Pharm Biopharm. 2009;72(2):289–94.

[2]. Pasparakis M, Haase I, Nestle FO. Mechanisms regulating skin immunity and inflammation. Nat Rev Immunol. 2014;14(5):289–301.

[3]. Kanitakis J. Anatomy, histology and immunohistochemistry of normal human skin. Eur J Dermatol. 2002;12(4):390–9.

[4]. Belkaid Y, Segre JA. Dialogue between skin microbiota and immunity. Science. 2014;346(6212):954–9.

[5]. Chehoud C, Rafail S, Tyldsley AS, Seykora JT, Lambris JD, Grice EA. Complement modulates the cutaneous microbiome and inflammatory milieu. Proc Natl Acad Sci U S A. 2013;110(37):15061–6.

[6]. Grice EA, Kong HH, Renaud G, Young AC, Bouffard GG, Blakesley RW, et al. A diversity profile of the human skin microbiota. Genome Res. 2008;18(7):1043–50.

[7]. Lai Y, Di Nardo A, Nakatsuji T, Leichtle A, Yang Y, Cogen AL, et al. Commensal bacteria regulate Toll-like receptor 3-dependent inflammation after skin injury. Nat Med. 2009;15(12):1377–82.

[8]. Shen W, Li W, Hixon JA, Bouladoux N, Belkaid Y, Dzutzev A, et al. Adaptive immunity to murine skin commensals. Proc Natl Acad Sci U S A. 2014;111(29): E2977–86.

[9]. Nagase N, Sasaki A, Yamashita K, Shimizu A, Wakita Y, Kitai S, et al. Isolation and species distribution of staphylococci from animal and human skin. J Vet Med Sci. 2002;64(3):245–50.

[10]. Tavakkol Z, Samuelson D, deLancey Pulcini E, Underwood RA, Usui ML, Costerton JW, et al. Resident bacterial flora in the skin of C57BL/6 mice housed under SPF conditions. J Am Assoc Lab Anim Sci. 2010;49(5):588–91.

[11]. Heath WR, Carbone FR. The skin-resident and migratory immune system in steady state and memory: innate lymphocytes, dendritic cells and T cells. Nat Immunol. 2013;14(10):978–85.

[12]. Nickoloff BJ, Turka LA. Immunological functions of non-professional antigen-presenting cells: new insights from studies of T-cell interactions with keratinocytes. Immunol Today. 1994;15(10):464–9.

[13]. Vono M, Lin A, Norrby-Teglund A, Koup RA, Liang F, Loré K. Neutrophils acquire the capacity for antigen presentation to memory CD4+ T cells in vitro and ex vivo. Blood. 2017;129(14):1991–2001.

[14]. Yang D, de la Rosa G, Tewary P, Oppenheim JJ. Alarmins link neutrophils and dendritic cells. Trends Immunol. 2009;30(11):531–7.

[15]. Gawriluk TR, Simkin J, Thompson KL, Biswas SK, Clare-Salzler Z, Kimani JM, et al. Comparative analysis of ear-hole closure identifies epimorphic regeneration as a discrete trait in mammals. Nat Commun. 2016; 7:11164.

[16]. Seifert AW, Kiama SG, Seifert MG, Goheen JR, Palmer TM, Maden M. Skin shedding and tissue regeneration in African spiny mice (Acomys). Nature. 2012;489(7417):561–5.

[17]. Godwin J. The promise of perfect adult tissue repair and regeneration in mammals: learning from regenerative amphibians and fish. Bioessays. 2014;36(9):861–71.

[18]. Godwin JW, Brockes JP. Regeneration, tissue injury and the immune response. J Anat. 2006;209(4):423–32.

[19]. Nodder S, Martin P. Wound healing in embryos: a review. Anat Embryol (Berl). 1997;195(3):215–28.

[20]. Cyr JL, Gawriluk TR, Kimani JM, Rada B, Watford WT, Kiama SG, et al. Regeneration-competent and -incompetent murids differ in neutrophil quantity and function. Integr Comp Biol. 2019;59(5):1138–49.

[21]. Gawriluk TR, Simkin J, Hacker CK, Kimani JM, Kiama SG, Ezenwa VO, et al. Complex tissue regeneration in mammals is associated with reduced inflammatory cytokines and an influx of T cells. Front Immunol. 2020; 11:1695.

[22]. Simkin J, Gawriluk TR, Gensel JC, Seifert AW. Macrophages are necessary for epimorphic regeneration in African spiny mice. eLife. 2017;6: e24623.

[23]. Belkaid Y, Hand TW. Role of the microbiota in immunity and inflammation. Cell. 2014;157(1):121–41.

[24]. Hand TW, Dos Santos LM, Bouladoux N, Molloy MJ, Pagán AJ, Pepper M, et al. Acute gastrointestinal infection induces long-lived microbiota-specific T cell responses. Science. 2012;337(6101):1553–6.

[25]. Linehan JL, Harrison OJ, Han SJ, Byrd AL, Vujkovic-Cvijin I, Villarino AV, et al. non-classical immunity controls microbiota impact on skin immunity and tissue repair. Cell. 2018;172(4):784–796.e18.

[26]. Naik S, Bouladoux N, Wilhelm C, Molloy MJ, Salcedo R, Kastenmuller W, et al. Compartmentalized control of skin immunity by resident commensals. Science. 2012;337(6098):1115–9.

[27]. Becker K, Heilmann C, Peters G. Coagulase-negative staphylococci. Clin Microbiol Rev. 2014;27(4):870–926.

[28]. Winn WC, Allen SD, Janda WM, Koneman EW, Procop GW, Schreckenberger PC, et al. Koneman's Color Atlas and Textbook of Diagnostic Microbiology. 6th ed. Philadelphia: Lippincott Williams & Wilkins; 2005.

[29]. Wilkinson HN, Hardman MJ. Wound healing: cellular mechanisms and pathological outcomes. Open Biol. 2020;10(9):200223.

[30]. Jackson RK. Unusual laboratory rodent species: research uses, care, and associated biohazards. ILAR J. 1997;38(1):13–21.

[31]. Baker DG. Natural pathogens of laboratory mice, rats, and rabbits and their effects on research. Clin Microbiol Rev. 1998;11(2):231–66.

[32]. Easterbrook JD, Kaplan JB, Glass GE, Watson J, Klein SL. A survey of rodent-borne pathogens carried by wild-caught

Norway rats: a potential threat to laboratory rodent colonies. Lab Anim. 2008;42(1):92–8.

[33]. Srinivas G, Möller S, Wang J, Künzel S, Zillikens D, Baines JF, et al. Genome-wide mapping of gene–microbiota interactions in susceptibility to autoimmune skin blistering. Nat Commun. 2013; 4:2462.

[34]. Belheouane M, Gupta Y, Künzel S, Ibrahim S, Baines JF. Improved detection of gene-microbe interactions in the mouse skin microbiota using high-resolution QTL mapping of 16S rRNA transcripts. Microbiome. 2017;5(1):59.

[35]. Garcia-Garcerà M, Garcia-Etxebarria K, Coscollà M, Latorre A, Calafell F. A new method for extracting skin microbes allows metagenomic analysis of whole-deep skin. PLoS One. 2013;8(9): e74914.

[36]. Grice EA, Kong HH, Renaud G, Young AC, NISC Comparative Sequencing Program, Bouffard GG, et al. A diversity profile of the human skin microbiota. Genome Res. 2008;18(7):1043–50.

[37]. Kloos WE, Bannerman TL. Update on clinical significance of coagulase-negative staphylococci. Clin Microbiol Rev. 1994;7(1):117–40.

[38]. Wang J, Kuenzel S, Baines JF. Draft genome sequences of 11 *Staphylococcus epidermidis* strains isolated from wild mouse species. Genome Announc. 2014;2(1): e01148–13.

[39]. Mescher AL, Neff AW, King MW. Inflammation and immunity in organ regeneration. Dev Comp Immunol. 2017; 66:98–110.

[40]. Simkin J, Gawriluk TR, Gensel JC, Seifert AW. Macrophages are necessary for epimorphic regeneration in African spiny mice. eLife. 2017;6: e24623.

[41]. Innerå M. Cutaneous vasculitis in small animals. Vet Clin North Am Small Anim Pract. 2013;43(1):113–34.

[42]. Kozlowski LM, Li W, Goldschmidt M, Levinson AI. In vivo inflammatory response to a prototypic B cell superantigen: elicitation of an Arthus reaction by staphylococcal protein A. J Immunol. 1998;160(11):5246–52.

[43]. Rajan TV. The Gell-Coombs classification of hypersensitivity reactions: a re-interpretation. Trends Immunol. 2003;24(7):376–9.

[44]. Cartin-Ceba R, Peikert T, Specks U. Pathogenesis of ANCA-associated vasculitis. Rheum Dis Clin North Am. 2010;36(3):463–77.

[45]. Muñoz-Grajales C, Pineda JC. Pathophysiological relationship between infections and systemic vasculitis. Autoimmune Dis. 2015; 2015:286783.

[46]. Arbiser JL, Dzieczkowski JS, Harmon JV, Duncan LM. Leukocytoclastic vasculitis following staphylococcal protein A column immunoadsorption therapy. Two cases and a review of the literature. Arch Dermatol. 1995;131(6):707–9.

[47]. Deodhar A, Allen E, Daoud K, Wahba I. Vasculitis secondary to staphylococcal Protein A immunoadsorption (Prosorba column) treatment in rheumatoid arthritis. Semin Arthritis Rheum. 2002;32(1):3–9

[48]. Baumann U, Chouchakova N, Gewecke B, Köhl J, Carroll MC, Schmidt RE, et al. Distinct tissue site-specific requirements of mast cells and complement components C3/C5a receptor in IgG immune complex-induced injury of skin and lung. J Immunol. 2001;167(2):1022–7.

[49]. Coxon A, Cullere X, Knight S, Sethi S, Wakelin MW, Stavrakis G, et al. FcγRIII mediates neutrophil recruitment to immune complexes: a mechanism for neutrophil accumulation in immune-mediated

inflammation. Immunity. 2001;14(6):693–704.

[50]. Mayadas TN, Tsokos GC, Tsuboi N. Mechanisms of immune complex-mediated neutrophil recruitment and tissue injury. Circulation. 2009;120(20):2012–24.

[51]. Clauss M, Sunderkötter C, Sveinbjörnsson B, Hippenstiel S, Willuweit A, Marino M, et al. A permissive role for tumor necrosis factor in vascular endothelial growth factor-induced vascular permeability. Blood. 2001;97(5):1321–9.

[52]. Sunderkötter C, Seeliger S, Schönlau F, Roth J, Hallmann R, Luger TA, et al. Different pathways leading to cutaneous leukocytoclastic vasculitis in mice. Exp Dermatol. 2001;10(6):391–404.

[53]. Anderson AL, Sporici R, Lambris J, Larosa D, Levinson AI. Pathogenesis of B-cell superantigen-induced immune complex-mediated inflammation. Infect Immun. 2006;74(2):1196–203.

[54]. Banaszkiewicz S, Wałecka-Zacharska E, Schubert J, Tabiś A, Król J, Stefaniak T, et al. Staphylococcal enterotoxin genes in coagulase-negative staphylococci—stability, expression, and genomic context. Int J Mol Sci. 2022;23(5):2560.

[55]. Park JY, Fox LK, Seo KS, McGuire MA, Park YH, Rurangirwa FR, et al. Detection of classical and newly described staphylococcal superantigen genes in coagulase-negative staphylococci isolated from bovine intramammary infections. Vet Microbiol. 2011;147(1–2):149–54.

[56]. Thonhofer R, Trummer M, Siegel C, Uitz E. Skin infection by coagulase negative staphylococci as a potential triggering factor for cutaneous leukocytoclastic vasculitis. Clin Med Arthritis Musculoskelet Disord. 2008; 1:1–4.

[57]. Vabulas RM, Bittlingmaier R, Heeg K, Wagner H, Miethke T. Rapid clearance of the bacterial superantigen staphylococcal enterotoxin B in vivo. Infect Immun. 1996;64(11):4567–73.

[58]. Zhao X, Chen J, Sun H, Zhang Y, Zou D. New insights into fibrosis from the ECM degradation perspective: the macrophage-MMP-ECM interaction. Cell Biosci. 2022;12(1):117.

[59]. Long H, Lichtnekert J, Andrassy J, Schraml BU, Romagnani P, Anders HJ. Macrophages and fibrosis: how resident and infiltrating mononuclear phagocytes account for organ injury, regeneration or atrophy. Front Immunol. 2023; 14:1268399.

Cite of article: Kimani JM, Kuria JKN, Kiama SG, Makanya AN. Immune response kinetics of the African Spiny Mouse (Acomys Percivali) To endogenous skin commensal infection: "rapid resolution of inflammation. Int. J. Med. Lab. Res. 2026; 11(2): 15-27. ***http://doi.org/10.35503/IJMLR.2026.11202***

CONFLICT OF INTEREST: Authors declared no conflict of interest
SOURCE OF FINANCIAL SUPPORT: Nil